Available online at www.sciencedirect.com
SCIENCE DIRECT®
GEODERMA
Geoderma 112 (2003) 179–196
www.elsevier.com/locate/geoderma

Hierarchical data fusion for mapping soil units at field scale

M. Sommer[a,*], M. Wehrhan[a], M. Zipprich[a], U. Weller[a], W. zu Castell[a], S. Ehrich[a], B. Tandler[a], T. Selige[b]

[a] *GSF—National Research Center for Environment and Health, Institute of Biomathematics and Biometry, Ingolstädter Landstraße 1, D-85764 Neuherberg, Germany*
[b] *Department of Plant Sciences, Chair of Plant Nutrition, Technical University Munich, Am Hochanger 2, D-85350 Freising, Germany*

Received 29 October 2001; accepted 14 October 2002

Abstract

We analyzed a highly complex soilscape of fluvial sediments by a hierarchical expert system. Using (i) inquiries, (ii) relief analysis on basis of a DEM 5, and (iii) soils' apparent electrical conductivity (EM38) as a database, we first defined zones of identical pedogenic context. Next, multi-temporal remote sensing data of winter wheat were obtained by an airborne multi-spectral scanner (Daedalus-ATM), which gives radiometric information with a geometric (ground) resolution of 1 m^2 (pixel size). Leaf area index (LAI) was semi-physically modeled using red and near-infrared canopy reflectances and related to above-ground biomass. Further, the resulting spatial patterns of vegetation parameters were processed by image analysis methods, i.e. an opening–closing procedure using a circular element with a radius of 5 m. These coarser patterns of LAI and biomass, respectively, were interpreted as patterns of site quality within each zone of pedogenic context. By our multi-temporal approach we were able to distinguish between stationary and time-variant pattern. Combined with point calibration on basis of a 50-m raster we identified available water capacity (AWC) and O_2 deficiency due to stagnant water as the most important soil properties constituting site quality for plant growth. Our results will be used for precision agriculture practices in future.

Keywords: Soil pattern; Relief analysis; EM38; Remote sensing; Expert systems

* Corresponding author. Tel.: +49-89-3187-2656; fax: +49-89-3187-3029.
E-mail address: sommer@gsf.de (M. Sommer).

0016-7061/02/$ - see front matter © 2002 Elsevier Science B.V. All rights reserved.
PII: S0016-7061(02)00305-1

1. Introduction

Precision agriculture evidently needs information about soil properties relevant for plant growth at a sub-field scale ($<10^2$ m extent). Because proper soil augering and complementary analysis at this scale would be too expensive, soil scientists are looking after low-cost, indirect methods to produce high-quality information about the relevant properties as well as their spatial extension. Most recently, remote sensing data, relief analysis on digital elevation models (DEM), as well as geophysical measures (ground-penetrating radar, electromagnetic induction) were used in this respect (Robert et al.,1999; Blackmore and Grenier, 2001). Relief analysis and geophysical methods are indirect methods for site quality and plant growth, respectively, which need additional pedo-transfer functions (PTF). Remote sensing of crop canopies can be directly related to plant canopy properties such as leaf area index (LAI), e.g. by a simplified modeling approach (Clevers, 1986). Spatial differences in LAI indicate soil-dependent site qualities, if other reasons, like pests, weeds or management failure can be excluded. But even then, the major problem in this "inverse interpretation" results from convergence phenomena (Schumm, 1991)—different (soil-related) causes may have the same effect. As an example, plant growth may be inhibited either by a smaller rooting depth (dense plough layers, acid subsoils, reductive horizons, etc.) or by the quality of that rooting volume (available water capacity (AWC), O_2 supply, nutrient contents, etc.). A functional analysis of the soilscape is needed to decipher the exact site-specific causes for differences in plant growth. Only a comprehensive understanding of the soil pattern yields a sound basis for adequate precision agriculture practices. Quantitative soil pattern analysis still is rather empirical and descriptive either by using geostatistics (e.g., Mausbach and Wilding, 1991), structural analysis (e.g., Fridland, 1976; Hole and Campbell, 1985) or hybrid techniques (reviewed in McBratney et al., 2000). On the landscape scale, we are far away from any thorough understanding of the underlying processes in time and space. First, very simplistic process models were published recently (Heimsath et al., 1997; Minasny and McBratney, 1999, 2001). On the other hand, the factorial approach (Jenny, 1941) has gained at least insight into the context of those processes, generally by comparative studies.

Here, we present an integrative method for soilscape analysis. A hierarchical expert system for multi-data fusion of inquiries, relief analysis, geophysical measurements (EM38) and remote sensing data was developed. In this respect, we combined the factorial theory of pedogenesis (Jenny, 1941) with the so-called "scaleway" of Roth et al. (1999). According to the latter, soil variability can be separated at every scale into a scale-typical, predictable part (structure) and a random part (texture), which becomes structure at the following subscale level. On field and landscape scale, structure results from pedogenesis and therefore from the soil forming factors, as it was demonstrated by numerous studies (reviewed in Birkeland, 1999; Sommer and Schlichting, 1997). In our model, the spatial variability of soil forming factors and their hierarchical impact on soils defines the pedogenic context for any site-specific interpretation of vegetation parameters [LAI, fresh and dry matter (FM and DM)], which were derived from multi-temporal remote sensing data. Results are presented from one field, A15, although the method is used in catchments as natural process units.

2. Materials and methods

2.1. Study area and soil forming factors

The study area is a field of 4.75 ha situated in the tertiary hilly landscape, 40 km north of Munich, Germany ("Klostergut Scheyern", 11°27′E, 48°30′N). Climate is characterized by a 30-year mean annual temperature of 7.4 °C and a 30-year mean annual precipitation of 803 mm. Rainfall and temperature during "vegetation periods" (defined for winter wheat as beginning October 1 until date of flight) are plotted in Fig. 1 for two selected years. The "vegetation period" of 1993/1994 (October 1, 1993–July 4, 1994) only received 75% of the rainfall in 1999/2000 (October 1, 1999–June 28, 2000). The air temperature (2 m) was 0.6 °C higher in 1993/1994 than in 1999/2000. Therefore, under a climatic perspective, the first year of investigation was much drier compared to the last year.

Because the time of soil development (approx. 10,000 years) and climate can be regarded as similar in our landscape, three soil forming factors (Jenny, 1941) determine the soil pattern: (i) man, (ii) relief, and (iii) parent material. Besides the actual agricultural practices, major human activities include mining of clay, sand and gravels, landfills, remediation of quarries and most recent changes in land use. Conversion of meadow to arable land, and vice versa, were very common during the last decades. Former hop garden with intensive fertilization (P) and use of Cu as fungicide are nowadays used as arable land as well. Old (analog) maps and inquiries are the exclusive tools to get information of the past land use.

Relief information was obtained by laser altimetry. The scattered data with a mean distance between measurement points of 3.7 m were resampled into a regular 5 × 5 m grid yielding a high precision DEM (DEM 5). Precision of the Laser-DEM 5 in height were

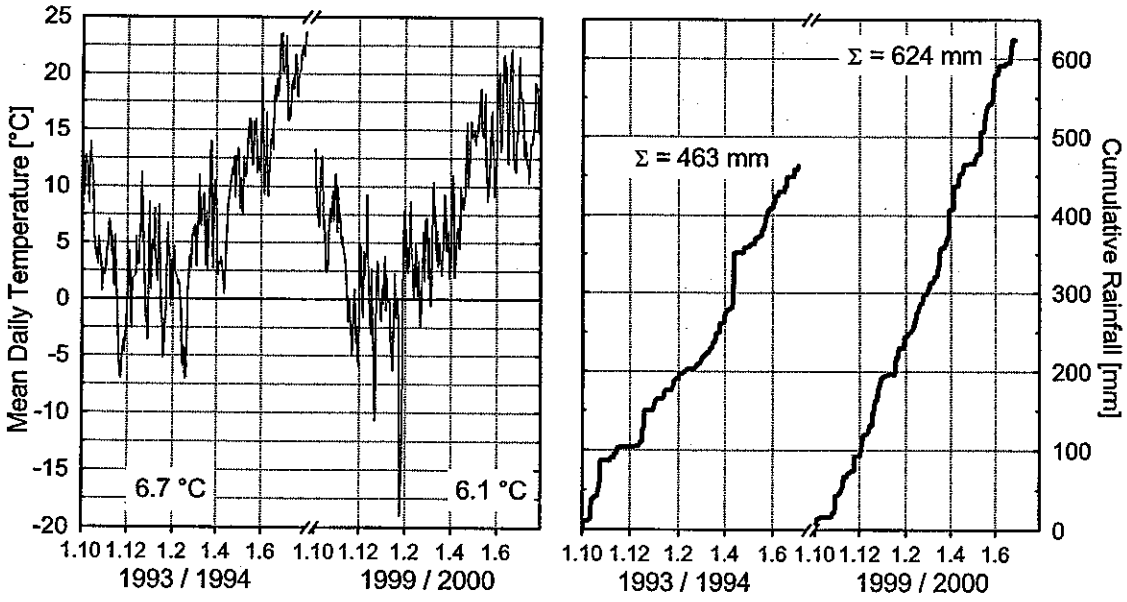

Fig. 1. Mean daily temperatures (left) and cumulative rainfall (right) of the weather station "Voglried" (data of station no. 070 from http://www.stmelf.bayern.de/lbp/agm/station/agm_start.html).

measured at a plain control surface and yielded a maximum over estimation of the height by +35 cm (mean deviation = – 0.3 cm, standard deviation = 7 cm, n = 496 points). Based on the DEM 5, different relief parameters were calculated with the software package System for Automated Relief Analysis (SARA, produced by Scilands, see http://www.scilands.de). Here, we only present the upslope catchment area of each grid cell and the slope curvature in three classes (concave, convex, linear).

The parent material of the study area is dominated by tertiary fluvial deposits showing the maximal possible span of textures (gravels to clays). Up to 3 m loess cover can be found on gentle east-facing slopes, while loess is missing on the steeper west-facing slopes (asymmetric valleys). The landscape was denuded through pleistocene solifluction as well as by holocene man-made erosion. A stratigraphic separation of tertiary and quaternary sediments was given by Sinowski and Auerswald (1999). From local pedogenic expert knowledge it is well known that redoximorphic soils (stagnant water soils = *Pseudogleys*) will develop preferably on loamy to clayey parent materials. One characteristic of these soils is the O_2 deficiency for plant growth in topsoils during wet seasons. On the other hand, nutrient and water supply will be enhanced on soils of fine-textured sediments compared to the coarser ones. So, we decided to separate at least two groups of parent materials, namely the sandy to gravelly from the loamy to clayey sediments. For this purpose, we used electromagnetic induction method.

2.2. Electromagnetic induction and interpolation

The apparent electrical conductivity (ECa) signal varies according to the amount of water and charged surfaces. The measuring device EM38 (Geonics) is installed on a wooden sledge, which can be pulled by tractor or even moved manually. This kind of measuring practice leads to sloping tracks of data locations. Our investigation is based on measurements carried out by Durlesser and Sperl (Durlesser, 1999), as well as Heil et al., 2001.

In addition to the ECa measurements, horizon-wise soil analyses on a 50 × 50 m grid all over the area of investigation are available (Sinowski, 1995; see also our Soil Information System at http://www.gsf.de/FAM/bis.html). To get a correlation between the ECa value and the clay content of the soil at each grid point, the integral of the convolution of the particle size mass distribution and the ECa signal density function was calculated. The particle size classes were calculated per soil volume (including the >2-mm fraction) and the horizon values weighted according to the vertical distribution of the signal density Ψ up to a depth of 1 m. Assuming a homogeneous conductor, the signal density at the depth z is calculated as (McNeill, 1980):

$$\Psi(z) = \frac{4z}{(4z^2 + 1)^{\frac{3}{2}}}. \quad (1)$$

For interpolation of the point data measured by the EM38 device, we used radial basis function (RBF) interpolation. In contrast to approximation, interpolation preserves the data values at the sampled locations and creates a smooth surface over the area. Using interpolation rather than approximation underlines our aim to separate the statistical

analysis from preconditioning the data. The assumption of second-order stationarity was doubted and kriging of the points led to very smooth interpolation surfaces.

Using RBFs for interpolation of scattered data is a standard technique in applied mathematics. The idea is to assume the interpolation function to be of the form

$$s(x) = \sum_{j=1}^{N} a_j \varphi(\|x - x^j\|_2), \quad x \in \mathbb{R}^2, \tag{2}$$

where φ: $\mathbb{R} \rightarrow \mathbb{R}$ is a so-called *radial basis function*. This approach reflects the idea of taking a function φ which is symmetric around the origin, and moving the function to the given data locations. Typical examples of basis functions are thin plate splines ($\varphi(r) = r^2 \log r$, $r \in \mathbb{R}_+$), multiquadrics ($\varphi(r) = \sqrt{c^2 + r^2}^{\beta}$, $r \in \mathbb{R}_+$, $c, \beta \in \mathbb{R}$) or gaussians ($\varphi(r) = \exp(-cr^2)$, $r \in \mathbb{R}_+$, $c > 0$). As all of those have global support, i.e., are non-zero on the whole positive axis, they lead to time-consuming calculations on large data sets. Therefore, a second class of basis functions having compact support have recently been introduced and investigated (cf. the survey by Buhmann, 2000).

Functions of this family typically are of the form

$$\varphi(r) = (1 - r)^{\beta} + p(r), \quad r \in \mathbb{R}_+, \beta > 0, \tag{3}$$

where p is some polynomial and $(r)_+ = r$, $r \geq 0$, and 0 else. Since the resulting matrices are sparse, these functions are more suitable for large data sets, although they are less accurate according to their order of approximation. In this example we used the function suggested by Wendland (1995), where $\beta = 4$ and $p(r) = 4r + 1$ in Eq. (3).

To analyze the data, we used the software package S+2000 to calculate the regressions. The procedures for RBF interpolation are taken from the package VISCAT, i.e., an interface of SINTEF's SISCAT library (Hjelle, 1996) to the GIS ArcView. The algorithms to calculate the selection procedures have been implemented as C^{++} programs.

2.3. Remote sensing

Multi-spectral imagery was acquired from winter wheat with a DAEDALUS AADS 1268 scanner on a DO 228 platform on July 4, 1994 and June 28, 2000 under optimum flight conditions. Flight altitude was 450 m above ground resulting in a geometric resolution of about 1 m. Geometric and radiometric corrections were applied involving the DEM 5. Differences in red and infrared reflectance of bare soil could be obtained from harvested fields in the surrounding of the research farm in order to check the assumptions made by Clevers (1986). An approximation for the infinite reflectance value was determined by using the maximum infrared reflectance within each field in order to minimize effects caused by radiometric disturbances, which could not be eliminated by correction procedures. Thus, the calculation of LAI was done for each individual field.

Ground truth was acquired at 23 representative sites from seven fields in 1994 and 26 sites from three fields in 2000 in order to cover the complete range of crop variables including LAI, FM and DM weight. LAI was measured with a LICOR plant canopy analyzer. Due to a disease in one field, five plots in 1994 were excluded from the LAI data

set. FM was ascertained by the sum of our samples of 0.25 m^2 each within an area of 25 m^2. Regression analysis was applied in order to ascertain DM weight from remotely sensed LAI values. DM weight is the sum of all assimilation processes during the vegetation period (Geisler, 1983) and thus a time-integrating indicator for the relation to soil properties, rather than LAI and FM, which may be influenced by actual water content due to varying short-time weather conditions.

2.3.1. Spectral characteristics of vegetation

Vegetation reflects incoming solar radiation in a characteristic manner (Fig. 2, left). In the visible region, reflectances are low because of absorption by chlorophyll pigments especially in the red domain. Transmittance is weak and almost no radiation penetrates inside the canopy after interception by the uppermost leaf layer. Therefore, the visible range is useful for estimating soil cover as soil reflectance is relatively high compared to vegetation (Clevers, 1986). In contrast, transmittance and reflectance increases rapidly in the near-infrared domain. Absorption is absent and canopy layers (and soil) underneath the upper layer contribute significantly to the total measured reflectance. This tends towards a limit termed "infinite reflectance" (Baret, 1991). The multiple reflectance in the near-infrared region appears to be a suitable estimator of LAI.

2.3.2. Model description

The physical relations describing the interception of solar radiation by a vegetation canopy and the subsequent scattering of radiation towards a sensor incorporates both, structural and optical properties of leaf layers and illumination and observation geometry. Most models have some simplifications of structural properties of the canopies architec-

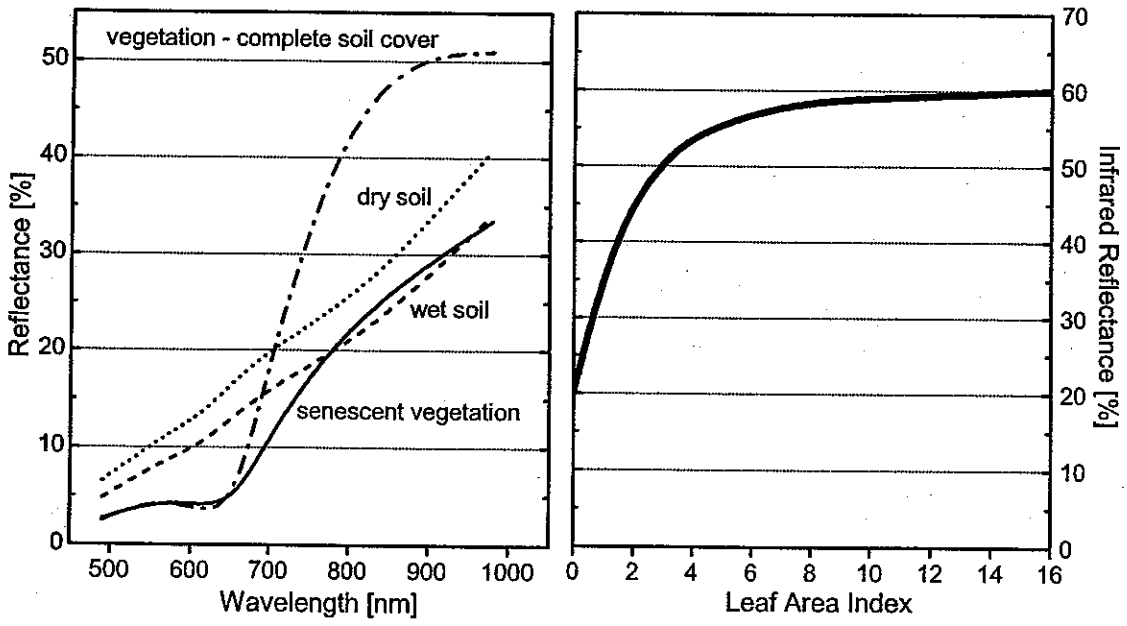

Fig. 2. Left: Spectral reflectance of vegetation (green and senescent) and soil with different moisture content in the visible and near-infrared region. Right: Near-infrared reflectance of vegetation (+soil) as a function of LAI. Adapted from Baret (1991).

ture in common. It is assumed that the canopy is infinitely extended horizontally and the single components are randomly and uniformly distributed within homogenous leaf layers. The Suits model uses the orthogonal projections of leaves in the horizontal and vertical plane as an approximation for the area of the original components that intercepts radiation. Furthermore, it is assumed that the projections of leaf normals are distributed uniformly in azimuth. Thus, the model simplifies the calculation of extinction coefficients by means of horizontally and vertically projected elements. From this model, Bunnik (cited in Clevers, 1986) deduced a relationship between infrared reflectance and LAI by means of a linear combination of several exponential functions incorporating canopy structure and scattering properties.

The general expression for a semiempirical model proposed by Baret (1991) is:

$$R = R_\infty + (R_s - R_\infty)e^{-K\mathrm{LAI}}, \tag{4}$$

where R is the total measured reflectance, R_∞ is the infinite reflectance value, R_s is the soil background reflectance and K is an extinction coefficient. All variables depend on wavelength and the parameters mentioned above. For an infrared passband, the shape of the relation between modeled LAI and reflectance resembles a "Mitscherlich curve" with three parameters (Clevers, 1986, Fig. 2, right).

If infrared reflectance can be corrected for soil background reflectance, only two parameters remain:

$$R'_{ir} = R_{\infty,ir}(1 - e^{-\alpha\mathrm{LAI}}), \tag{5}$$

where R'_{ir} is the corrected infrared reflectance, $R_{\infty,ir}$ is the infinite reflectance value in the infrared region and α is a combination of extinction and scattering coefficients. The LAI is then calculated by the inverse of eq. (5):

$$\mathrm{LAI} = \frac{-1}{\alpha}\ln\left(1 - \frac{R'_{ir}}{R_{\infty,ir}}\right). \tag{6}$$

Values for α were adapted from Clevers (1986) who estimated them from a training set on winter wheat fields in the generative stage of development, which is comparable with the phenological situation in this study.

2.3.3. Correction for soil background reflectance

Before estimating the LAI from Eq. (6), a correction for soil background reflectance has to be applied to an infrared passband. The main assumption is that there is a constant ratio between reflectances of bare soil in different passbands, independent of soil moisture content. This should also be true for the difference in reflectances between a red and an infrared passband. If soil reflectance is known (which is not strictly demanded), the corrected infrared reflectance (applied, e.g. to a red passband) can be approximated by

$$R'_{ir} = R_{ir} - \frac{R_{s,ir}(R_r - R_{v,r})}{(R_{s,r} - R_{v,r})} \tag{7}$$

Table 1
Reflectances (infinite, soil) and α for estimating LAI

Date	$R_{\infty,ir}$	α	$R_{s,r}$	$R_{s,ir}$
July 4, 1994	52.52	0.33	19.36	38.57
June 28, 2000	55.85	0.33	22.42	37.35

Field A15 in 1994 and 2000.

where $R_{s,ir}$ is the infrared reflectance of the soil, R_r is the total red reflectance, $R_{s,r}$ is the red reflectance of the soil, and $R_{v,r}$ is the red reflectance of the vegetation. Clevers used calculations of Verhoef's SAIL model to compare them with the results of his simplified approach. The agreements were satisfyingly high.

Values for $R_{\infty,ir}$, α and soil reflectances in 1994 and 2000 for A15 are given in Table 1.

2.3.4. Filtering of remote sensing data

The estimated spatial distribution of the DM, as displayed by an image, exhibits heterogeneities on a wide variety of scales. They are caused by a variety of influences. For interpretation, we were interested in soil-related structures at a scale of >10 m extent (pedotopes). Therefore, we had to eliminate linear, man-made structures like tractor lanes as well as short-ranged heterogeneities. Additionally, the technical options of precision agriculture are limited to that scale at the moment.

The images were filtered by a non-linear operator that is formed by a series of opening/closing–closing/opening procedures. The filtering element was a circular disc whose radius was increased stepwise leading to a series of images with larger and larger heterogeneities eliminated. Opening is defined as an erosion operation followed by a dilation (i.e., $O=DE$). Erosion means that a filtering element (usually a disc of a given size) is placed on the point and that the point is assigned the maximum value within the filtering element. In other words, given a set of pairs $\{(v_i,x_i): i=1,\ldots,N\}$ where v_i is a data value and the x_i are Euclidean coordinates in the plane, erosion with a disc of radius r can be written as:

$$E(v_i) = \max_{x_j \in B_r(x_i)} v_j \text{ with } B_r(x_i) = \{x \in \mathbb{R}^2: \ \|x - x_i\|_2 \leq r\}. \tag{8}$$

Dilation is the same but with the minimum operator instead of the maximum. Closing is the opposite operation of opening (i.e., $C=ED$). Opening eliminates each dark heterogeneity smaller than the filtering element while leaving bright structures untouched, and closing eliminates the bright structures. The combined use of opening and closing has a comparable effect on the images as a median filter. In a stricter sense, median filtered values always lie between OC and CO filtered (Rohwer, 1998). The advantage is that bright and dark structures can be separated and that the minimum/maximum operations are faster and easier to implement than median calculation. In contrast to these non-linear filters, linear filters like moving average do not properly eliminate the structures regarded but smear them over a larger area.

Table 2
Inputs for soil map unit delineation

Variable	Database and method
Man	Inquiries
Relief	DEM 5 + Relief analysis (SARA)
Parent material	ECa + Interpolation Methods (radial basis function) + raster point information (Soil Information System)
Soil pattern	Remote sensing (Daedalus AADS 1268) + filtering + raster point information (Soil Information System) + local expert knowledge

An overview of the methods and databases used gives Table 2.

3. Results and discussion

3.1. The pedogenic context

We developed a specific hierarchy of soil forming factors for our study area, which results from local expert knowledge. An increasing influence on soils and, consequently, on site properties can be stated as follows: man>relief>parent material. Hierarchy in this sense means a change in a factor on higher hierarchical level has a greater impact on soil pattern, regardless of differences in low level factors. Consequently, each class of high

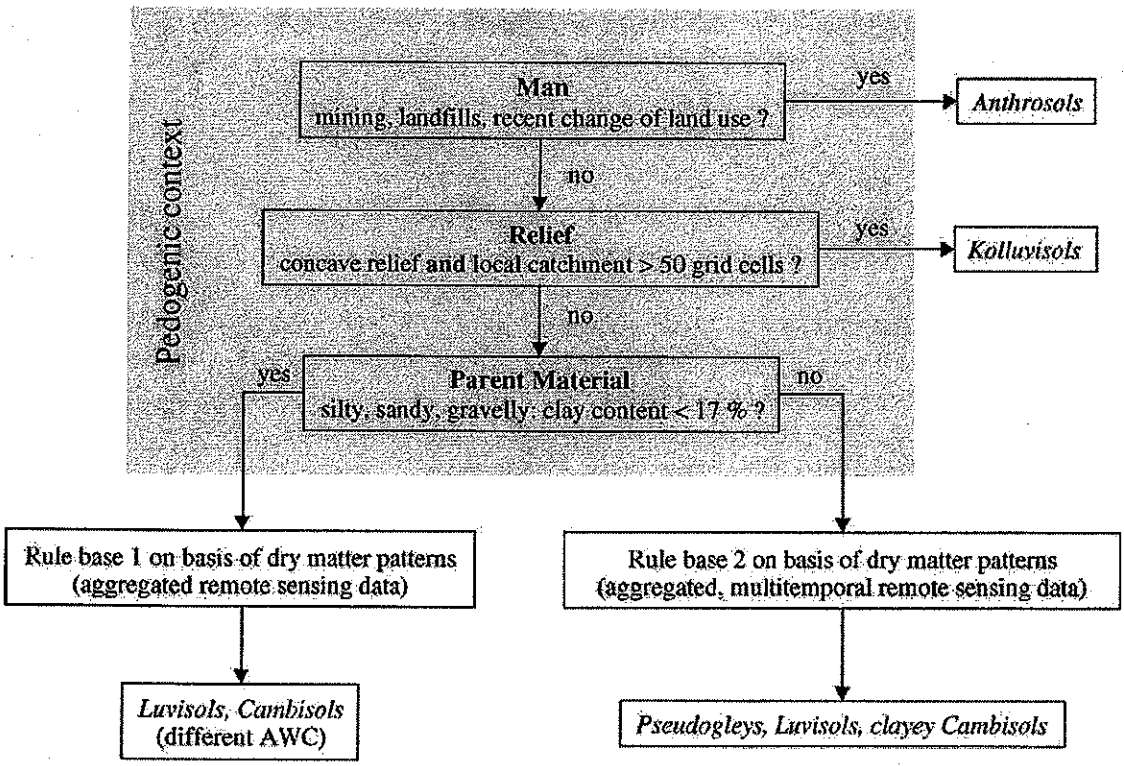

Fig. 3. General framework of hierarchical rule-based system for multi-data fusion.

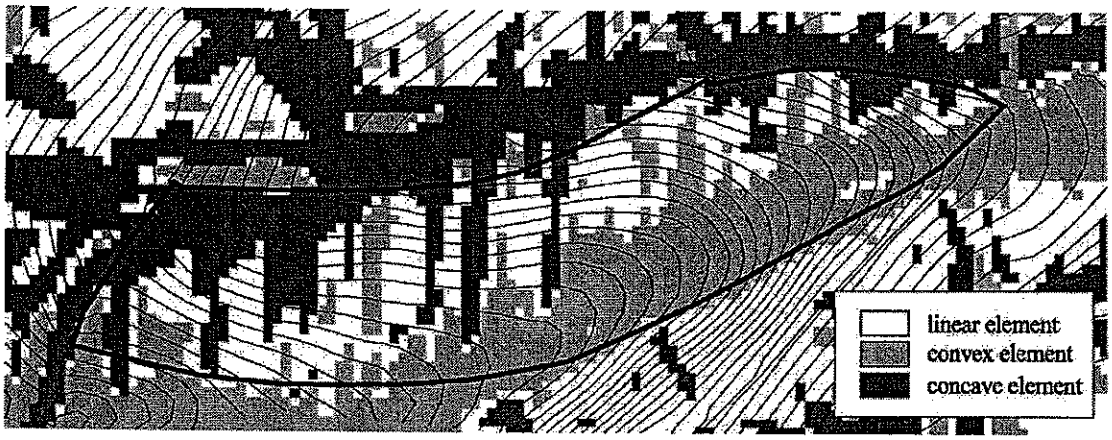

Fig. 4. Slope curvature of A15 on basis of DEM 5; dark grey = concave relief elements (convergent surface water flow), light grey = convex relief elements (divergent surface water flow).

ranking factors constitutes a new context for changes in sublevel factors. Through this procedure, the entire landscape is split up into sets of different pedogenic context by a decision tree (Bui and Moran, 2001). The general framework of this hierarchical rule-based system is shown in Fig. 3.

3.1.1. Man and relief

According to our inquiries, there was no major human impact at our field A15. Therefore, we do not need to differentiate the field in respect to this soil forming factor. Relief is controlling the superficial water and sediment transport through differences in gravitation potentials. Concave parts of the landscape will slow down the transport of water–sediment suspensions and consequently enhance sedimentation (= colluviation). In addition, a certain catchment area is needed for any substantial amount of sediment. Colluviated sites will receive additional water and nutrient inputs and, therefore, will be sites of high plant biomass. We used relief parameters derived from relief analysis as proxies for the location and geometry of colluvial sites. Concave relief elements were more frequent in the (flatter) western part of A15 (Fig. 4). This zone also showed higher values for the local catchment areas (Fig. 5). Expert knowledge of the soilscape and calibration on the 50 m raster data set leads to the following rule: Pixels will be regarded as *Kolluvisols*[1] whenever they belong to a concave landscape position and show a local catchment area of at least 50 grid cells. At A15, only small portions of the field belong to this soil type (Fig. 5, hatched).

3.1.2. Parent material

The EM38 data set was gathered at anisotropic locations with a short measuring distance within the tracks of measurement and a larger gap between them. Therefore, the data could be thinned out according to a quality criterion with respect to the interpolation error. Note that theoretical error bounds show that thinning out carefully does not much influence the accuracy of the interpolation function, but leads to much faster calculations for large data

[1] In the German Classification System (DBG, 1998), *Kolluvisols* are characterized by a colluvial layer ("M" horizon) of at least 40 cm.

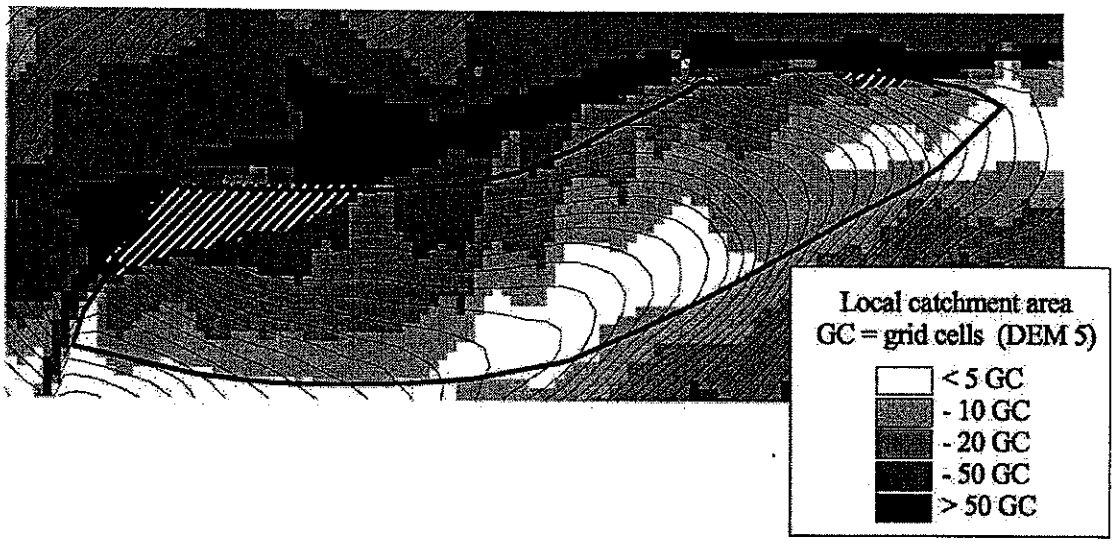

Fig. 5. Local catchment areas of A15, hatched areas = *Kolluvisols* at A15.

sets. The removed sets of approximately 250 points could then be used to optimize the radius of the RBF by calculating the mean absolute error at these points. Fig. 6 (left) shows an increase of the error for large values of the radius. This is due to the fact that RBF problems become numerically unstable as the support of the function rises. Our experiment showed that a radius of approximately five times the track distance (e.g., 75–80 m for A15) leads to optimal interpolation functions, although a large range of radii gave approximately equal results. The interpolation was then performed using the whole set of points with a radius of 80 m.

The correlation of the interpolated apparent soil conductivities ECa with soil textural properties was investigated at raster points. The strongest correlation exists between log(ECa) and the weighted clay content of total soil, i.e., including the >2-mm fraction (Fig. 6, right, Eq. (9)).

$$\text{Clay } [\%] = -0.52 + 0.47\log_{10}(\text{ECa}),\ r^2 = 0.81,\ n = 15,\ P < 0.001. \tag{9}$$

Consideration of the dry bulk density does not improve r^2. The r^2 value found in our investigation is slightly higher compared to those found by other authors (Schmidhalter et al., 2001: $r^2 = 0.31–0.67$, Dalgaard and Have, 2001: $r^2 = 0.79$), which is assumed to be caused by the larger range (6–41%) of weighted clay content at our sample locations.

For the interpretation of the results, we assumed that the intensity of pedogenic clay (neo-)formation to be negligible compared to the (huge span of) parent material textures. This is reasonable for all sediments in the study area, except loess. Furthermore, we did not interpret the ECa pattern as total, but only the pattern of values above and below a certain threshold. Below 17% clay[2] sandy and gravelly tertiary fluvial deposits (*Molasse*) will occur, above that value loamy to clayey tertiary sediments (*Molasse*) as well as (non-eroded) loessial soils. Fig. 7 shows the steps from the measured point data via interpolation to the distinction of two textural classes. The eastern part of field A15 is dominated by the

[2] The boundary equals the textural boundary of sands in the German Soil Classification System.

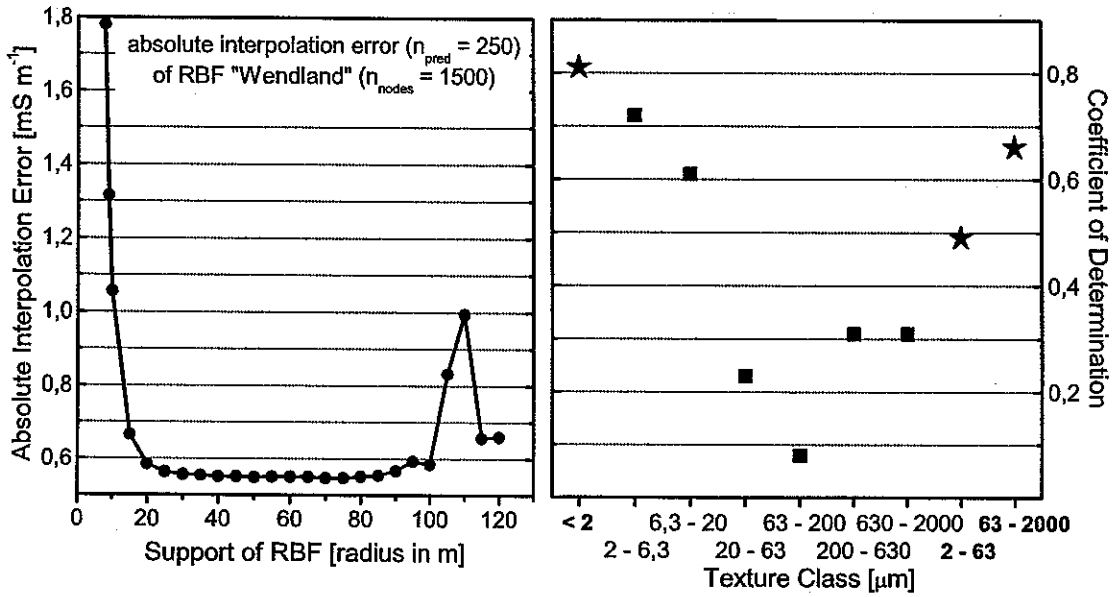

Fig. 6. Left: Interpolation error as function of radius. Right: correlations between texture classes and log(ECa).

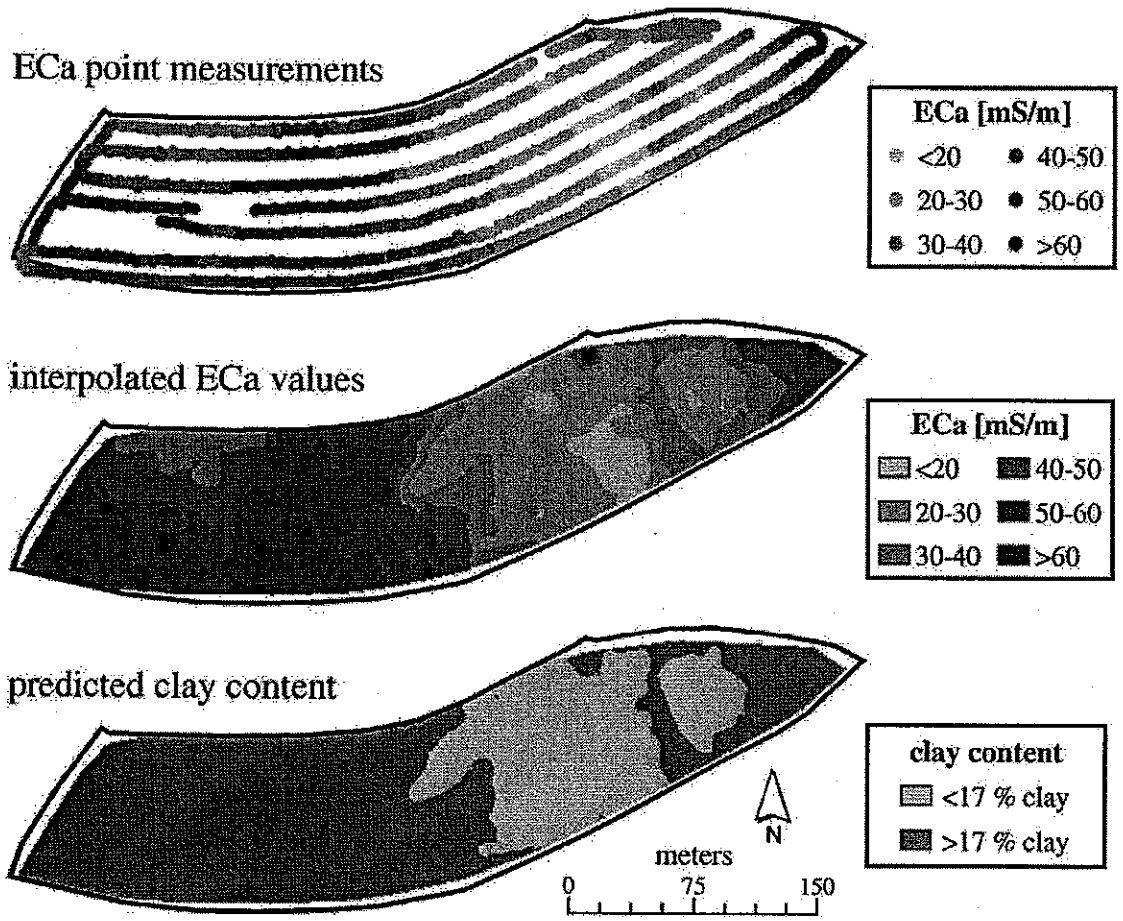

Fig. 7. Upper: ECa point measurements; middle: interpolated values (Wendland function, radius 80 m); lower: pattern of parent material according to the clay threshold value.

sandy to gravelly *Molasse*, whereas soils of the western part developed from loamy to clayey *Molasse* as well as from loess.

3.2. LAI and biomass pattern

Clevers' approach was applied to all winter wheat fields on the research farm. The results for field A15 represent well the overall range of LAI from below 1 up to a maximum values of 12 (only a few pixel) in both years. It is obvious that the spatial pattern remains more or less constant (Fig. 8). Differences in absolute LAI mainly appear in the eastern and western parts of the field. The eastern part is dominated by a certain shift towards higher values in 2000 (wet year). In the western sector, the area with lower LAI values increases significantly.

The regressions of estimated LAI values on measured FM as well as FM on DM are shown in Fig. 9. The relationship between estimated LAI and FM remains more or less constant although different Ground Truth plots were used. Although FM and DM are strongly related in each year, a distinct shift appears between the 2 years caused by differences in water and nutrient supply during the vegetation period (Fig. 9, right).

The wheat DM differed by a factor of 2.5 (max.) for both years, which indicates huge differences in site quality at A15. The medians of DM were similar in both years (1994: 1.12; 2000: 1.23 kg m^{-2}). Compared to the warmer and drier period (1994), the wetter and cooler year (2000) showed a greater spreading of DM (Fig. 10, upper). Aggregation procedure eliminated the small linear structures at A15 (tractor lanes), but did not change the range of values and pattern (compare Fig. 10, middle and lower). However, we have to

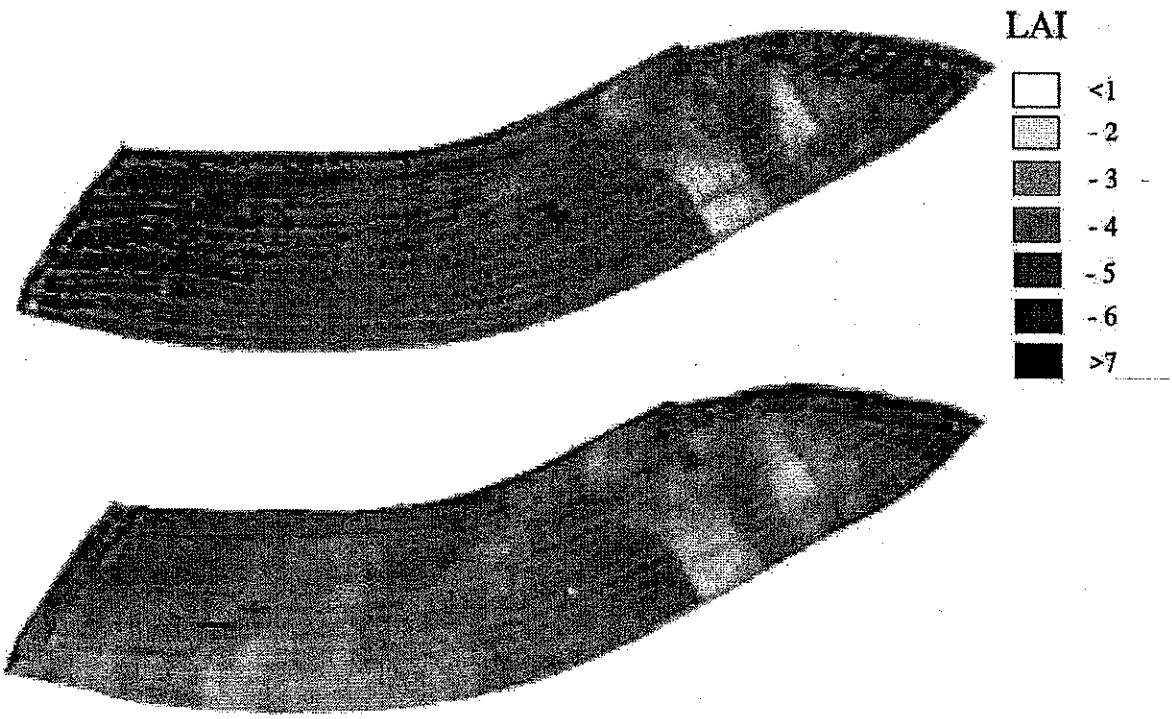

Fig. 8. Estimated leaf area index of field A15 for 2 years. Upper: July 4, 1994; lower: June 28, 2000.

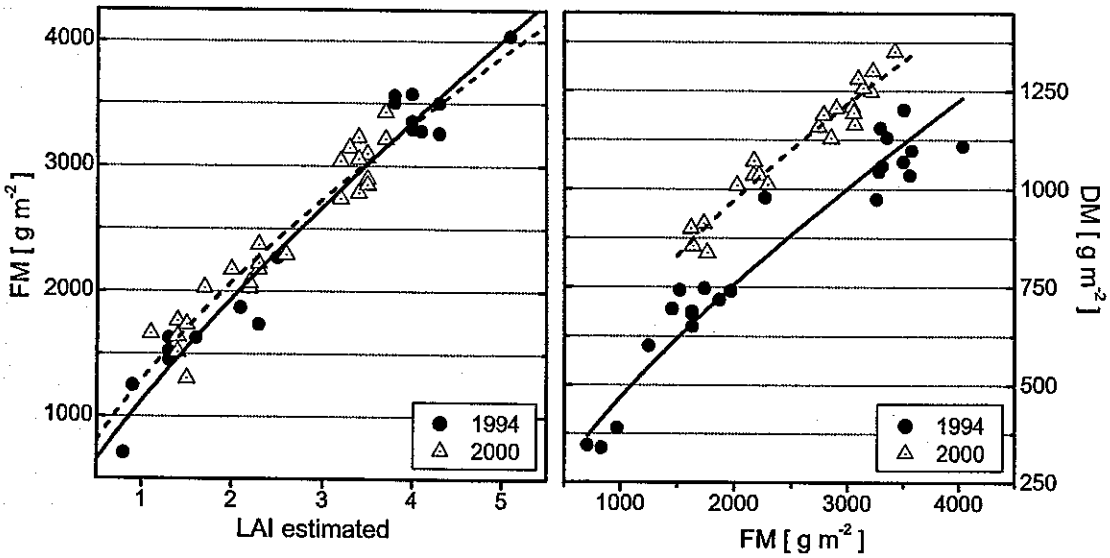

Fig. 9. Left: Regression of estimated LAI on measured fresh matter. Right: Regression of fresh matter on measured dry matter.

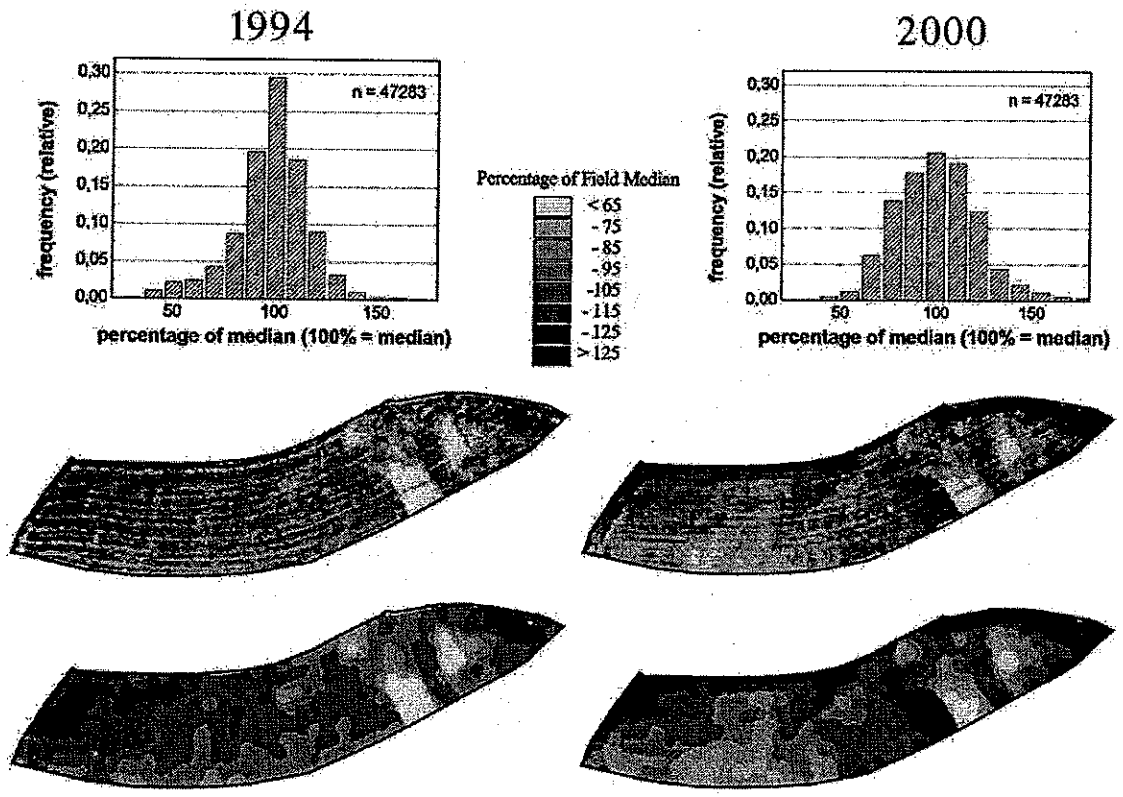

Fig. 10. Upper: Frequency distributions of non-aggregated dry matter. Middle: Non-aggregated pattern of dry matter as percentages of field median. Lower: Aggregated pattern of dry matter as percentages of field median (opening–closing procedures with circular element $r = 5$ m).

note a "rounding effect" on the pattern due to the shape of the filter itself. We could distinguish between stationary, time-invariant patterns and non-stationary, time-variant types (Fig. 10, lower). Obviously, low biomass structures developed at same spots in the eastern part of A15 (sandy to gravelly parent material, compare Fig. 7) regardless of the climatic situation. In the western part of A15 (loamy to clayey parent material, compare Fig. 7), structures of highest biomass can be regarded as stationary as well. In contrast, structures of very low biomass developed only in wet and cool 2000. Additionally, pattern seemed to be arranged catenary in this part of A15.

3.3. Soil pattern and properties

The biomass pattern observed can be related to soils with the help of the 50-m raster data set. According to their recording in an earlier research phase, sampling points were not ideally placed for any calibration purpose (Fig. 11). Nevertheless, we developed our rule base on the 50-m raster basis. The resulting spatial pattern will be validated through transect augerings. For the area of sandy to gravelly Molasse, we defined three soil units by the following threshold values (year 2000): sites with extremely low DM (<85% of field median) were separated from patches of intermediate (85–105%) and high DM (105–125%; nos. 1–3 in Fig. 11). As expected, no stagnant water soils appeared in this part of the field; instead, the silt content increased with increasing wheat biomass and, therefore, the loess influence. Silt content, on the other hand, has a strong influence on the water supply of soils, especially the AWC (Renger, 1971). Consequently, highest biomasses (>125% of field median) corresponded to non-redoximorphic soils developed almost exclusively from loess (=soil unit 4). For the remainder area of loamy to clayey sediments, three soil units of decreasing stagnant water influence can be deciphered: (i) lowest biomasses (<85%) were found at *Pseudogleys* (redoximorphic features <50 cm

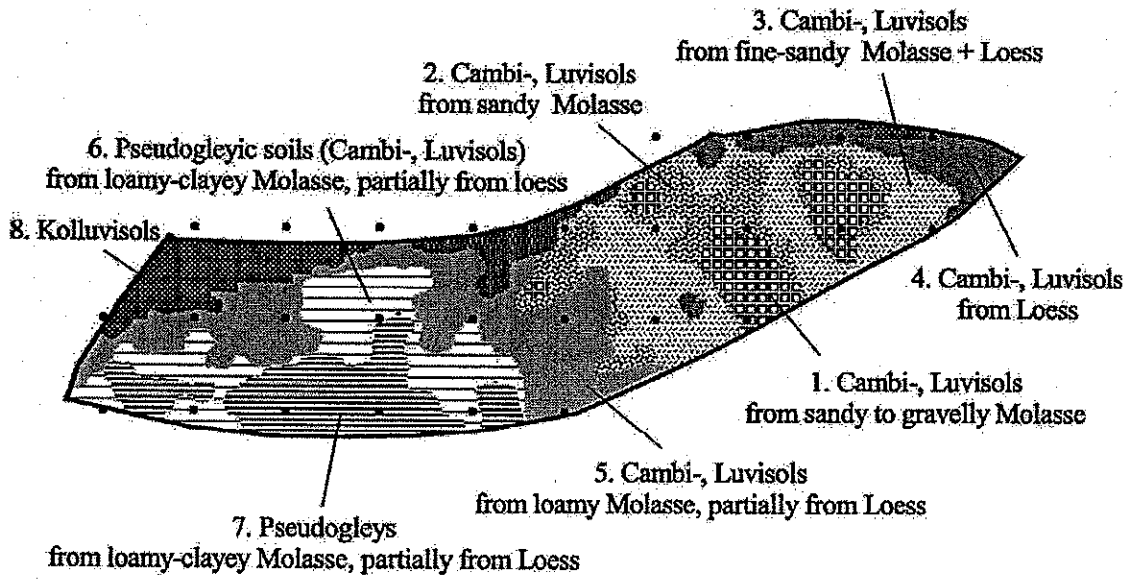

Fig. 11. Soil map units of A15; points=calibration points of the 50-m raster; straight boundaries between units results from the coarser resolution of the DEM 5/EM38 measurements compared to remote sensing data.

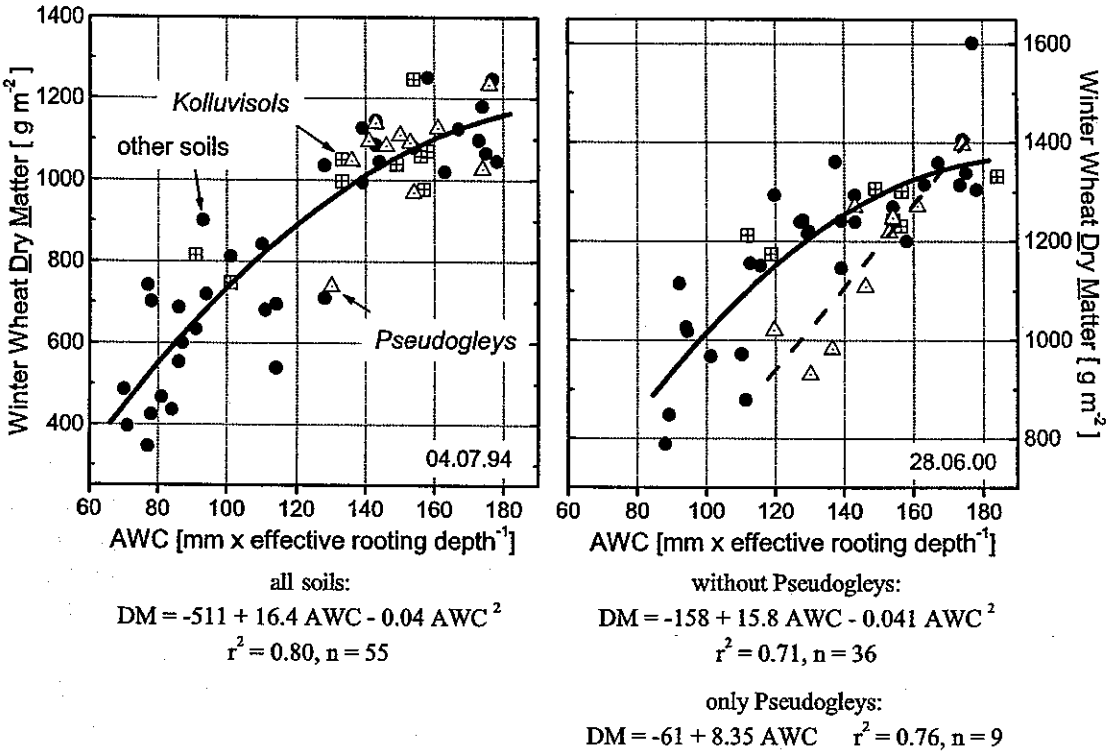

Fig. 12. Relationship between available water capacity (pF1.8–pF4.2) and winter wheat dry matter in 1994 (left) and 2000 (right); data from all 50-m raster points of all fields in a single year.

depth, soil unit 5); (ii) intermediate values (85–95%) at pseudogleyic sites (redoximorphic features 50–100 cm, soil unit 6); and (iii) sites with wheat DM at and slightly above field median (95–115%) showed no redoximorphic features in the upper meter (soil unit 7). As expected, colluvial sites (soil unit 8) matched areas of high DM (>115%).

Our analysis of the soilscape and the resulting plant reaction lead us to the hypothesis of **plant available water** to be the most prominent influencing factor on plant growth (compare Runge and Hons, 1999). Therefore, we plotted AWC vs. DM of winter wheat for both years. As can be seen from Fig. 12, there is a non-linear relationship between both variables (Selige, 1997). In a dry year (1994), no differentiation between soils can be stated; whereas in a wetter year (2000), the *Pseudogleys* showed lower DM values. This fits very well with our hypothesis on the importance of anaerobic conditions in stagnant water soils during wet periods. Therefore, temporal O_2 deficiency for roots is the next important factor of site quality in our study area. Because *Pseudogleys* behave like other soils in normal and dry years, their areas can only be delineated in wet years. Consequently, for these soils a multi-temporal remote sensing approach is needed.

4. Conclusions

With the help of relief analyses and electromagnetic induction, a pedogenic context for soil pattern development can be defined. Thus, we avoided convergence phenomena interpreting the remote sensing data. Airborne remote sensing of plant canopies is a

powerful tool for both, precision agriculture and soil science. Vegetation parameters, like LAI or biomass, can be imaged with a high spatial resolution at field scale. These data may be used for an estimation of yield as well as for cultivation practices. Given a defined context of soil forming factors, the geometry of vegetation parameters from remote sensing can also be translated into soil patterns and properties. The advantage of the method developed lies in the area-wide information—no interpolation, but reasonable aggregation is needed. There is no need to seek for the exact geometry of hidden soil units. Instead, areas of similar plant response must be filled with soil science knowledge. Additionally, the use of multi-temporal remote sensing data allows analysts to identify soils and soil properties, which are very important for plant growth, but which cannot be deduced from other non-invasive methods. The methodology requires further validation, which will be carried out in three steps: (i), it will be checked whether the predictions of soils in the cores of the identified zones are correct; (ii) a catenary study has to show the validity of the predicted soil gradients; and (iii) the overall areal topology of the soil associations has to be analysed and compared to the model prediction.

Acknowledgements

This work was performed in the 'Research Network Agroecosystems Munich' (FAM) and financed by the BMBF.

References

Baret, F., 1991. Vegetation canopy reflectance: factors of variation and application for agriculture. In: Belward, A., Valenzuela, R. (Eds.), Rem. Sens. and Geographical Information Systems for Resource Management in Developing Countries. ECSE, EEC, EAEC, Brussels, pp. 145–167.

Birkeland, P., 1999. Soils and Geomorphology. Oxford Univ. Press, Oxford.

Blackmore, S., Grenier, G. (Eds.), 2001. Third European Conference on Precision Agriculture 2001. Full Paper CD. Agro Montpellier, Ecole Nationale Superieur Agronomique, Montpellier.

Buhmann, M.D., 2000. Radial basis functions. Acta Numer. (9), 1–38.

Bui, E., Moran, C., 2001. Disaggregation of polygons of surficial geology and soil maps using spatial modelling and legacy data. Geoderma 103, 79–94.

Clevers, J.G.P.W., 1986. Application of remote sensing to agricultural field trials. Vol. 86 of Agricultural University Wageningen Papers. Agricultural University Wageningen.

Dalgaard, M., Have, H., 2001. In: Blackmore, Grenier (Eds.), Soil Clay Mapping by Measurement of Electromagnetic Conductivity, pp. 367–372.

DBG, 1998. Systematics of soils and soil forming substrates of Germany (in German). Mitteilungen. Dtsch. Bodenkundl. Gesell., vol. 86. German Soil Science Society.

Durlesser, H.P., 1999. Determination of the Variation of Soil Physical Parameters Through Time and Space by Electromagnetic Induction (in German). Shaker, Aachen.

Fridland, V.M., 1976. Pattern of Soil Cover. Israel Program for Scientific Translation, Jerusalem.

Geisler, G., 1983. Yield Physiology of Cultivated Plants of the Temperate Climate (in German). Verlag Paul Parey, Berlin.

Heimsath, A.M., Dietrich, W.E., Nishiizumi, K., Finkel, R., 1997. The soil production function and landscape equilibrium. Nature 388, 358–361.

Hjelle, Ø., 1996. Explicit surfaces in Siscat. The Siscat Report Series. SINTEF, Oslo.

Hole, F.D., Campbell, J., 1985. Soil Landscape Analysis. Routledge and Kegan Paul, London.

Jenny, H., 1941. Factors of Soil Formation. McGraw-Hill, New York.
Mausbach, M.J., Wilding, L. (Eds.), 1991. Spatial Variabilities of Soils and Landforms. SSSA Spec. Publ., vol. 28. SSSA, Madison, WI.
McBratney, A.B., Odeh, I.O.A., Bishop, T.F.A., Dunbar, M.S., Shatar, T.M., 2000. An overview of pedometric techniques for use in soil survey. Geoderma 97, 293–327.
McNeill, J.D., 1980. Electromagnetic Terrain Conductivity Measurement at Low Induction Numbers. Mississauga, Ontario.
Minasny, B., McBratney, A.B., 1999. A rudimentary mechanistic model for soil production and landscape development. Geoderma 90, 3–21.
Minasny, B., McBratney, A.B., 2001. A rudimentary mechanistic model for soil production and landscape development: II. A two-dimensional model incorporating chemical weathering. Geoderma 103, 161–180.
Renger, M., 1971. The estimation of pore size distribution from texture, organic matter content and bulk density (in German). Z.Pflanzenern. Bodenk. 130, 53–67.
Robert, P.C., Rust, R.H., Larson, W.E. (Eds.), 1999. Proceedings of the 4th International Conference on Precision Agriculture. Part A and B. ASA, CSSA, SSSA, Madison, WI.
Rohwer, C., 1998. Idempotent one-side approximation of median smoothers. J. Approx. Theory 58 (2).
Roth, K., Vogel, H.-J., Kasteel, R., 1999. The scaleway: a conceptual frame-work for upscaling soil properties. In: Feyen, J., Wiyo, K. (Eds.), Modelling of Transport in Soils. Wageningen Press, Wageningen, pp. 477–490.
Runge, E.C.A., Hons, F.M., 1999. Precision agriculture—development of a hierarchy of variables influencing crop yields. In: Robert, et al. (Eds.), pp. 143–158.
Schmidhalter, U., Zintel, A., Neudecker, E., 2001. Calibration of electromagnetic induction measurements to survey the spatial variability of soils. In: Blackmore, Grenier (Eds.), pp. 479–484.
Schumm, S.A., 1991. To Interpret the Earth—Ten Ways to be Wrong. Cambridge Univ. Press, Cambridge.
Selige, T., 1997. Remote sensing and relief analysis as tools for agricultural site assessment (in German). In: Felix-Henningsen, P., Wegener, H.-R. (Eds.), Boden Landsch., vol. 17. University of Giessen, pp. 121–138.
Sinowski, W., 1995. The Three-Dimensional Ariability of Soil Properties (in German). Shaker, Aachen.
Sinowski, W., Auerswald, K., 1999. Using relief parameters in a discriminant analysis to stratify geological areas with different spatial variability of soil properties. Geoderma 89, 113–128.
Sommer, M., Schlichting, E., 1997. Archetypes of catenas in respect to matter—a concept for structuring and grouping catenas. Geoderma 76, 1–33.
Wendland, H., 1995. Piecewise polynomial, positive definite and compactly supported radial functions of minimal degree. Adv. Comput. Math. 4, 389–396.

Jenny, H., 1941. Factors of Soil Formation. McGraw-Hill, New York.
Mausbach, M.J., Wilding, L. (Eds.), 1991. Spatial Variabilities of Soils and Landforms. SSSA Spec. Publ., vol. 28. SSSA, Madison, WI.
McBratney, A.B., Odeh, I.O.A., Bishop, T.F.A., Dunbar, M.S., Shatar, T.M., 2000. An overview of pedometric techniques for use in soil survey. Geoderma 97, 293–327.
McNeill, J.D., 1980. Electromagnetic Terrain Conductivity Measurement at Low Induction Numbers. Mississauga, Ontario.
Minasny, B., McBratney, A.B., 1999. A rudimentary mechanistic model for soil production and landscape development. Geoderma 90, 3–21.
Minasny, B., McBratney, A.B., 2001. A rudimentary mechanistic model for soil production and landscape development: II. A two-dimensional model incorporating chemical weathering. Geoderma 103, 161–180.
Renger, M., 1971. The estimation of pore size distribution from texture, organic matter content and bulk density (in German). Z.Pflanzenern. Bodenk. 130, 53–67.
Robert, P.C., Rust, R.H., Larson, W.E. (Eds.), 1999. Proceedings of the 4th International Conference on Precision Agriculture. Part A and B. ASA, CSSA, SSSA, Madison, WI.
Rohwer, C., 1998. Idempotent one-side approximation of median smoothers. J. Approx. Theory 58 (2).
Roth, K., Vogel, H.-J., Kasteel, R., 1999. The scaleway: a conceptual frame-work for upscaling soil properties. In: Feyen, J., Wiyo, K. (Eds.), Modelling of Transport in Soils. Wageningen Press, Wageningen, pp. 477–490.
Runge, E.C.A., Hons, F.M., 1999. Precision agriculture—development of a hierarchy of variables influencing crop yields. In: Robert, et al. (Eds.), pp. 143–158.
Schmidhalter, U., Zintel, A., Neudecker, E., 2001. Calibration of electromagnetic induction measurements to survey the spatial variability of soils. In: Blackmore, Grenier (Eds.), pp. 479–484.
Schumm, S.A., 1991. To Interpret the Earth—Ten Ways to be Wrong. Cambridge Univ. Press, Cambridge.
Selige, T., 1997. Remote sensing and relief analysis as tools for agricultural site assessment (in German). In: Felix-Henningsen, P., Wegener, H.-R. (Eds.), Boden Landsch., vol. 17. University of Giessen, pp. 121–138.
Sinowski, W., 1995. The Three-Dimensional Ariability of Soil Properties (in German). Shaker, Aachen.
Sinowski, W., Auerswald, K., 1999. Using relief parameters in a discriminant analysis to stratify geological areas with different spatial variability of soil properties. Geoderma 89, 113–128.
Sommer, M., Schlichting, E., 1997. Archetypes of catenas in respect to matter—a concept for structuring and grouping catenas. Geoderma 76, 1–33.
Wendland, H., 1995. Piecewise polynomial, positive definite and compactly supported radial functions of minimal degree. Adv. Comput. Math. 4, 389–396.